Earthquakes and Structures, *Vol. 18, No. 2 (2020) 171-184*
DOI: https://doi.org/10.12989/eas.2020.18.2.171

Mitigation of seismic collision between adjacent structures using roof water tanks

Sayed Mahmoud*

Department of Civil and Construction Engineering, College of Engineering, Imam Abdulrahman Bin Faisal University, Saudi Arabia

(*Received September 4, 2019, Revised November 18, 2019, Accepted November 19, 2019*)

Abstract. The potential of using the roof water tanks as a mitigation measure to minimize the required separation gap and induced pounding forces due to collisions is investigated. The investigation is carried out using nonlinear dynamic analysis for two adjacent 3-story buildings with different dynamic characteristics under two real earthquake motions. For such analysis, nonlinear viscoelastic model is used to simulate forces due to impact. The sloshing force due to water movement is modelled in terms of width of the water tank and the instantaneous wave heights at the end wall. The effect of roof water tanks on the story's responses, separation gap, and magnitude and number of induced pounding forces are investigated. The influence of structural stiffness and storey mass are investigated as well. It is found that pounding causes instantaneous acceleration pulses in the colliding buildings, but the existence of roof water tanks eliminates such acceleration pulses. At the same time the water tanks effectively reduce the number of collisions as well as the magnitude of the induced impact forces. Moreover, buildings without constructed water tanks require wider separation gap to prevent pounding as compared to those with water tanks attached to top floor under seismic excitations.

Keywords: pounding; seismic gap; sloshing force; inelastic response; earthquake

1. Introduction

Insufficiently separated adjacent structures with different dynamic characteristics pound together due to out of phase vibration under seismic excitations. Pounding between neighboring structures is classified as one of the reasons causing damage during earthquakes (Rosenblueth and Meli 1985, Kasai and Maison 1997, GRM 2009). For the past few decades, structural pounding attracted many researchers in order to evaluate the seismic performance of adjacent structures during collisions. Pounding between adjacent buildings with fixed-bases as well as buildings with isolated-bases has been extensively investigated (Anagnostopoulos 1988, Komodromos *et al*. 2007, Jankowski 2008, Mahmoud and Jankowski 2010, Mahmoud and Gutub 2013, Mahmoud and Abdelhameed 2013). Several improvements in design codes have been introduced in order to prevent occurrence of pounding or reducing the level of damage due to such complex phenomena. Researchers focused on the concept of interconnecting adjacent buildings with active, passive, semi-active and smart damping control devices to reduce induced responses and consequently collisions between such buildings under dynamic lateral loads. Such installed devices can be used to control both displacement and acceleration responses. Connecting insufficiently separated adjacent buildings with linking elements in the form of springs, dashpots, or viscoelastic is another strategy to mitigate and reduce earthquake-induced pounding (Jankowski and Mahmoud 2016). Abdel-Mooty and Ahmed (2017) introduced a mitigation approach in order to reduce pounding and minimize the developed force between existing neighboring buildings or building parts separated by expansion or structural joints. The mitigation approach proposes a localized linking of building parts in one line or forming L-shape. A coupling strategy with the use of magneto-rheological (MR) damper only at top floor has been utilized for the purpose of reducing collisions between planar buildings with different dynamic characteristics and insufficiently separated (Abdeddaim *et al*. 2016). Four different control strategies, namely: passive-off, passive-on, semi-active on-off controller and fuzzy logic controller have been compared to assess the performance of the MR for pounding hazard mitigation and the coupled system in terms of the induced story displacement, drift, and acceleration responses. Anagnostopoulos and Karamaneas (2008) proposed a practical solution to the separation gap between adjacent buildings recommended by modern seismic design codes in which collision shear walls acting transversely as bumper-type are used to minimize damage of contacting buildings during collisions.

Tuned mass dampers (TMDs), as passive control devices, are commonly used to enhance the induced structural responses through a system of springs and dashpots that connects an auxiliary mass to the main structure. Abdullah *et al*. (2001) proposed a shared TMD to control the vibrations of adjacent structures and to reduce the probability of occurrence of pounding. Magneto-rheological (MR) dampers, as semi-active devices, are widely used to control vibrations of civil structures under

*Corresponding author, Associate Professor
E-mail: elseedy@hotmail.com
E-mail: smabdein@iau.edu.sa

Copyright © 2020 Techno-Press, Ltd.

ISSN: 2092-7614 (Print), 2092-7622 (Online)

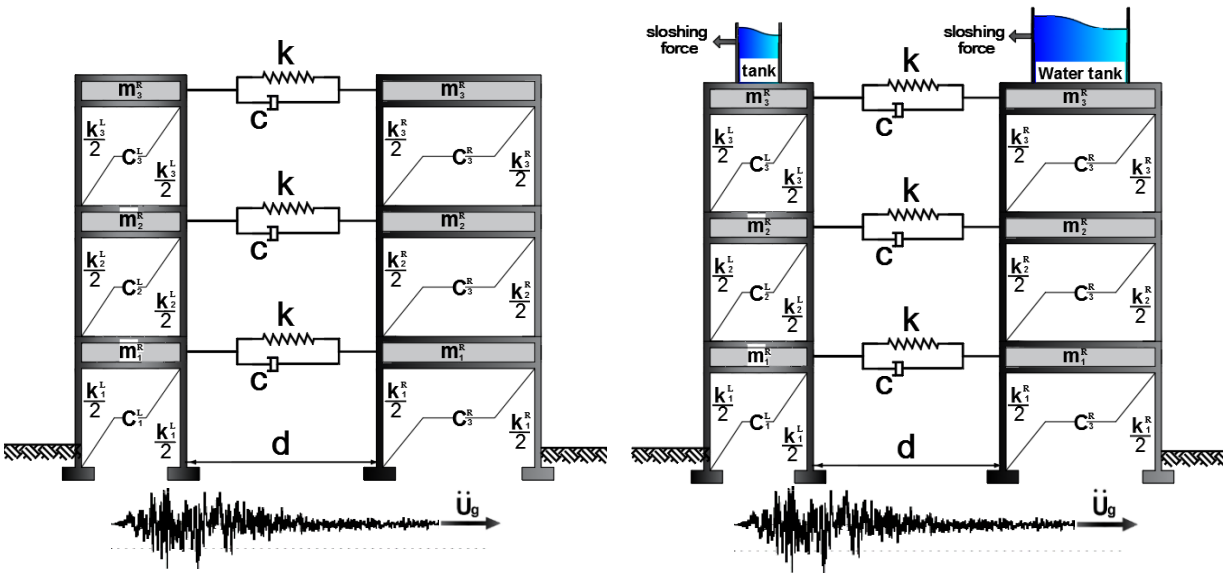

Fig. 1 Schematic diagram of adjacent three-story buildings (a) without water tanks, and (b) with water tanks at top floors

seismic actions (Dyke *et al*. 1998). Guenidi *et al*. (2017) controlled the responses of two adjacent buildings following two strategies. The first strategy through employing a shared TMD and second one with hybrid system combining a classic TMD and MR damper. Cao and Li (2019) are the first to propose tuned tandem mass dampers-inerters (TTMDI) by integrating the tuned tandem mass dampers (TTMD) with two inerters for the mitigation of undesirable oscillations of buildings under earthquake excitations.

Most of the performed research analysis on structural pounding consider the storey levels of the adjacent and insufficiently separated structures always the same in order to ensure avoiding inter-story pounding. Karayannis and Favvata (2005b) are the first among others to introduce the concept of inter-storey pounding through examining the effect of collisions between insufficiently separated structures with unequal heights on the ductility requirements and the overall seismic response of reinforced concrete structures. the results of the performed study clearly indicated that the impacted columns develop shear strength requirements of higher values that exceed the allowable columns capacity and high ductility demand as well. Karaiance and Naoum (2018) expected the occurrence of a potential local shear brittle failure at specified time periods when the developed shear force exceeds the available shear capacity. Neglecting inter-story pounding may lead to non-conservative or even hazardous building design (Karayannis and Favvata 2005a).

Karaiance and Naoum (2018) expected the occurrence of a potential local shear brittle failure at specified time periods when the developed shear force exceeds the available shear capacity. Neglecting inter-story pounding may lead to non-conservative or even hazardous building design. Karayannis and Favvata (2005a) examined the influence of collisions between adjacent multi-storey reinforced concrete buildings considering the two distinct types of pounding problem in terms of collisions at level of storey masses as the first type and between slabs and columns as the second type of pounding. The study concluded that ignorance of the possible effects of pounding leads to non-conservative building design or evaluation particularly for the second scenario in which impacting occurs between slabs and columns. This may help improving the seismic design codes to assist in the building design process. Although masonry infill is considered as non-structural elements, it has a substantial effect on the global seismic performance of building structures where the captured response of building models with masonry infill do significantly vary compared with bare building models. Based on such significant influence of the infill walls on the dynamic behaviour of building structures, Favvata *et al*. (2009) performed an analysis to investigate the influence of the masonry infill on seismic interaction between insufficiently separated adjacent buildings in terms of the critical column and the exterior joints that suffers the impacting effect. However, due to the complexity of the process of modelling masonry infill especially for lumped mass parameters models as in the current study and uncertainties associated with infill walls as non-structural elements, the influence of the masonry infill is usually ignored in the modelling and design process (Mahmoud *et al*. 2017, Elwardany *et al*. 2017, Abdel Raheem *et al*. 2018a)

Water tanks offers benefits of low cost and minimal maintenance over time as compared to auxiliary damping systems. This paper assesses the performance of water tanks attached at the top floors in counteracting motions of adjacent structures insufficiently separated under earthquake loads. Two different configurations are considered; adjacent buildings with attached water tanks at top floors and adjacent buildings without. The nonlinear viscoelastic model is used to simulate the pounding forces between stories of buildings under two strong ground motion records. The obtained seismic responses of both buildings in terms of story displacement, acceleration, and pounding force are presented for the considered two configurations.

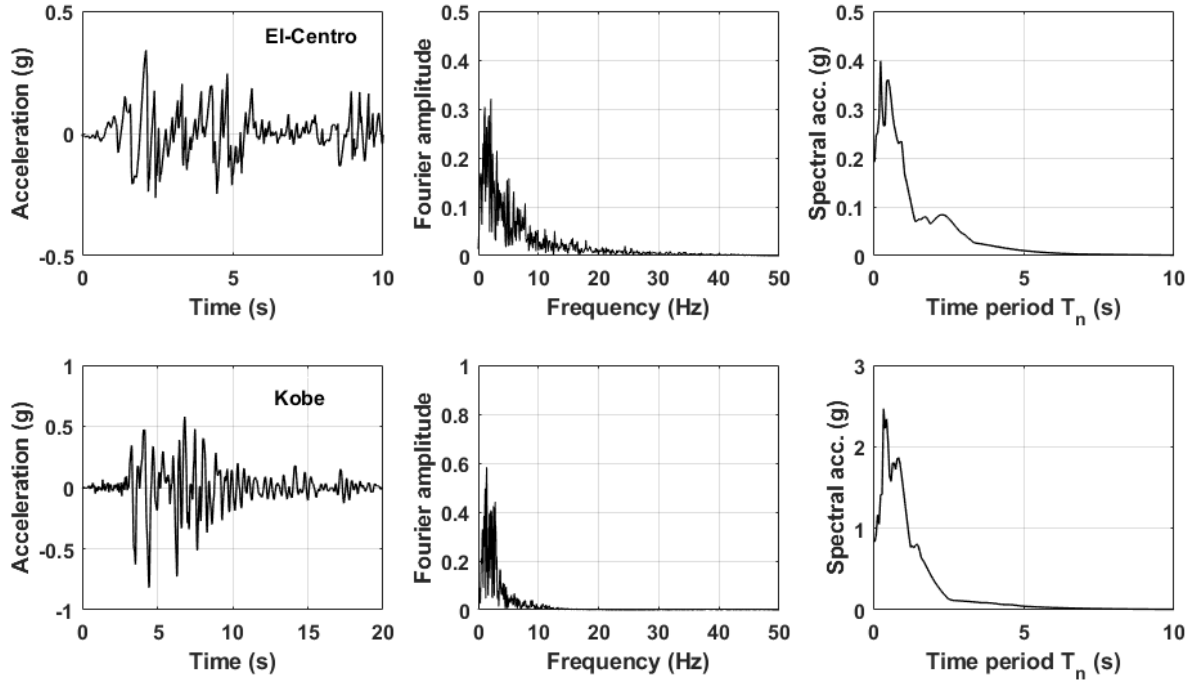

Fig. 2 Acceleration time histories, Fourier transform signals, and acceleration response spectra at 5% critical damping for the El-Centro and Kobe ground motion records

2. Adjacent buildings model

Two adjacent three-story buildings modeled as shear building type are considered in the present study. The masses of the superstructure are lumped at each story level with one lateral degree of freedom corresponding to the floor level. The schematic diagram of the adjacent three-story buildings without and with roof water tanks is shown in Fig. 1, where m_i^L, m_i^R; c_i^L, c_i^R; and ; k_i^L, k_i^R (i=1, 2, 3) respectively denote the masses, damping and stiffness coefficients of the left and right buildings. The details of the governing equations of motions for the considered adjacent building models are described in Section 4.

3. Earthquake input excitation

The adjacent building models with and without roof water tanks shown in Fig. 1 were excited by two earthquake records from 1940 El-Centro, and 1995 Kobe. The recorded stations of the records are 117 El Centro and KJMA. The chosen ground excitation records for performing the simulation analysis differ in their peak ground accelerations (PGAs), magnitudes and site-source distances. the selected records are characterized with Magnitudes of *Mw*=7.2 and *Mw*=6.9 for the El-Centro and Kobe respectively. Fig. 2 presents the selected two earthquake records as the acceleration time histories and Fourier transform signals. In addition, the acceleration response spectra at 5% critical damping is also presented. The simulation time of the two earthquakes are 10 and 20 seconds for the El-Centro and Kobe records respectively. The well-known site of Berkeley University namely; PEER Strong Motion Database, was utilized to obtain the earthquake records used for performing the simulation analysis. (http://peer.berkeley.edu/smcat/).

4. Governing equations of motion

This section presents the coupled equations of motion of the building models shown in Fig. 1 considering and ignoring the effect of sloshing force due to the application of seismic loads.

4.1 Equations of motion ignoring sloshing force

The dynamic equation of motion of the building models presented in Fig. 1(a) during collisions can take the form

$$\begin{pmatrix} \boldsymbol{M^L} & \boldsymbol{O} \\ \boldsymbol{O} & \boldsymbol{M^R} \end{pmatrix}\begin{pmatrix} \ddot{\boldsymbol{U}}^{\boldsymbol{L}} \\ \ddot{\boldsymbol{U}}^{\boldsymbol{R}} \end{pmatrix} + \begin{pmatrix} \boldsymbol{C^L} & \boldsymbol{O} \\ \boldsymbol{O} & \boldsymbol{C^R} \end{pmatrix}\begin{pmatrix} \dot{\boldsymbol{U}}^{\boldsymbol{L}} \\ \dot{\boldsymbol{U}}^{\boldsymbol{R}} \end{pmatrix} + \begin{pmatrix} \boldsymbol{R^L} \\ \boldsymbol{R^R} \end{pmatrix} + \begin{pmatrix} \boldsymbol{P} \\ -\boldsymbol{P} \end{pmatrix} = -\begin{pmatrix} \boldsymbol{M^L} & \boldsymbol{O} \\ \boldsymbol{O} & \boldsymbol{M^R} \end{pmatrix}\begin{pmatrix} \ddot{\boldsymbol{U}}_{\boldsymbol{g}} \\ \ddot{\boldsymbol{U}}_{\boldsymbol{g}} \end{pmatrix} \quad (1)$$

where $\boldsymbol{M^L}$ and $\boldsymbol{C^L}$ represent the mass and damping coefficient matrices for the left building respectively. Similarly, $\boldsymbol{M^R}$ and $\boldsymbol{C^R}$ respectively denote the mass and damping coefficient matrices for the right building. $\boldsymbol{U^L}$, $\dot{\boldsymbol{U}}^{\boldsymbol{L}}$, $\ddot{\boldsymbol{U}}^{\boldsymbol{L}}$ and $\boldsymbol{U^R}$, $\dot{\boldsymbol{U}}^{\boldsymbol{R}}$, $\ddot{\boldsymbol{U}}^{\boldsymbol{R}}$ are vectors representing stories responses of the left and right buildings respectively in terms of displacement, velocity, and acceleration. $\boldsymbol{R^L}$ and $\boldsymbol{R^R}$ refer to the inelastic resisting forces of the left and right buildings system; the vector $\boldsymbol{P}$ indicates the induced pounding forces during collisions at each storey level; $\ddot{\boldsymbol{U}}_{\boldsymbol{g}}$ is the vector of the applied ground accelerations.

The matrices $\boldsymbol{M^L}$, $\boldsymbol{M^R}$, $\boldsymbol{C^L}$, $\boldsymbol{C^R}$ and $\boldsymbol{O}$ in terms of

elements of storey masses and damping coefficients of left and right buildings respectively can take the form

$$\boldsymbol{M}^{L}=\begin{pmatrix} m_1^L & 0 & 0 \\ 0 & m_2^L & 0 \\ 0 & 0 & m_3^L \end{pmatrix}, \boldsymbol{M}^{R}=\begin{pmatrix} m_1^R & 0 & 0 \\ 0 & m_2^R & 0 \\ 0 & 0 & m_3^R \end{pmatrix}, \quad \boldsymbol{O}=\begin{pmatrix} 0 & 0 & 0 \\ 0 & 0 & 0 \\ 0 & 0 & 0 \end{pmatrix} \tag{2a}$$

$$\mathbf{C}^{\mathrm{L}}=\begin{pmatrix} \mathrm{c}_1^{\mathrm{L}}+\mathrm{c}_2^{\mathrm{L}} & -\mathrm{c}_2^{\mathrm{L}} & 0 \\ -\mathrm{c}_2^{\mathrm{L}} & \mathrm{c}_2^{\mathrm{L}}+\mathrm{c}_3^{\mathrm{L}} & -\mathrm{c}_3^{\mathrm{L}} \\ 0 & -\mathrm{c}_3^{\mathrm{L}} & \mathrm{c}_3^{\mathrm{L}} \end{pmatrix}, \quad \boldsymbol{C}^{R}=\begin{pmatrix} c_1^R+c_2^R & -c_2^R & 0 \\ -c_2^R & c_2^R+c_3^R & -c_3^R \\ 0 & -c_3^R & c_3^R \end{pmatrix} \tag{2b}$$

The inelastic resisting force of the system $\boldsymbol{R^L}$ and $\boldsymbol{R^R}$ can be written in the vector form as

$$\boldsymbol{R}^{L}=\begin{pmatrix} R_1^L-R_2^L \\ R_2^L-R_3^L \\ R_3^L \end{pmatrix}, \boldsymbol{R}^{R}=\begin{pmatrix} R_1^R-R_2^R \\ R_2^R-R_3^R \\ R_3^R \end{pmatrix}, \tag{2c}$$

R_i^L and R_i^R can be defined in terms of initial stiffness coefficients k_i^R and k_i^L, displacements u_i^L and u_i^R and yield forces f_{yi}^L and f_{yi}^R $(i = 1,2,3)$ of the left and right buildings respectively as $R_i^L = k_i^L(u_i^L - u_{i-1}^L)$, $R_i^R = k_i^R(u_i^R - u_{i-1}^R)$ during the elastic stage and as $R_i^L = \pm f_{yi}^L$, $R_i^R = \pm f_{yi}^R$ during the plastic stage.

The vectors $\dot{\boldsymbol{U}}^{\boldsymbol{L}}$, $\dot{\boldsymbol{U}}^{\boldsymbol{R}}$, $\ddot{\boldsymbol{U}}^{\boldsymbol{L}}$, and $\ddot{\boldsymbol{U}}^{\boldsymbol{R}}$ which contains the storey velocity $\dot{u}_i^L$, $\dot{u}_i^R$; and acceleration $\ddot{u}_i^L$, $\ddot{u}_i^R$ can take the form

$$\dot{\boldsymbol{U}}^{L}=\begin{pmatrix} \dot{u}_1^L \\ \dot{u}_2^L \\ \dot{u}_3^L \end{pmatrix}, \dot{\boldsymbol{U}}^{R}=\begin{pmatrix} \dot{u}_1^R \\ \dot{u}_2^R \\ \dot{u}_3^R \end{pmatrix}, \ddot{\boldsymbol{U}}^{L}=\begin{pmatrix} \ddot{u}_1^L \\ \ddot{u}_2^L \\ \ddot{u}_3^L \end{pmatrix}, \ddot{\boldsymbol{U}}^{R}=\begin{pmatrix} \ddot{u}_1^R \\ \ddot{u}_2^R \\ \ddot{u}_3^R \end{pmatrix} \tag{2d}$$

The vector $\boldsymbol{P}$ that contains the induced forces due to collisions at each storey level and the right-hand side vector $\ddot{\boldsymbol{U}}_{\boldsymbol{g}}$ of the applied ground accelerations can take the vector form

$$\boldsymbol{P}=\begin{pmatrix} P_{11} \\ P_{22} \\ P_{22} \end{pmatrix}, \ddot{\boldsymbol{U}}_{\boldsymbol{g}}=\begin{pmatrix} \ddot{u}_g \\ \ddot{u}_g \\ \ddot{u}_g \end{pmatrix} \tag{2e}$$

Usually the inelastic nature of pounding phenomenon could directly be modelled through bilinear spring gap model with energy dissipation through hysteretic behaviour or indirectly through equivalent damping through dashpot (Mostafa and Mahmoud 2013, Abdel Raheem 2014, Karayannis and Naoum 2018). In the current study, the developed formulation considers the impact between the two neighbouring buildings by introducing a nonlinear spring in conjunction with a nonlinear viscous dashpot between the colliding structures which accounts for the inelastic nature through the equivalent damping of dashpot (Abdel Raheem *et al*. 2018b).

In order to model the induced forces due to collisions between the storeys of insufficiently separated adjacent buildings, the non-linear viscoelastic model, (see Jankowski 2005), which is commonly used in capturing forces due to pounding and also considered as one of the accurate models compared to others in capturing pounding forces, is utilized in the current study. The model consists of nonlinear spring and viscous impact dashpot elements. Two stages namely approaching, and restitution stages are defined to calculate impacting forces whenever there are impacts. The pounding force at time t and the i[th] (i = 1, 2, 3) story level can be written as (Jankowski 2005)

$$\begin{aligned} P_{ii} &= \bar{\beta}\delta_i^{\frac{3}{2}} + \bar{c}\dot{\delta}_i \quad \text{for } \delta_i > 0 \text{ and} \\ \dot{\delta}_i(t) &> 0 \quad (\text{contact} - \text{approachperiod}) \\ P_{ii} &= \bar{\beta}\delta_i^{\frac{3}{2}} \quad \text{for } \delta_i > 0 \text{ and} \\ \dot{\delta}_i(t) &\le 0 \quad (\text{contact} - \text{restitutionperiod}) \\ P_{ii} &= 0 \quad \text{for } \delta_i \le 0 \quad (no \text{ contact}) \end{aligned} \tag{3}$$

$\delta_i(t) = (u_i^l - u_i^r - d)$ and $\dot{\delta}_i(t) = (\dot{u}_i^l - \dot{u}_i^r)$ respectively define the relative displacement and relative velocity between the colliding i[th] stories with separation gap d. $\bar{\beta}$ and $\bar{c}$ are impact stiffness and damping coefficient parameters of the impact elements.

Recently, Karayannis and Naoum (2018) used different stiffness values to assess their influence on the induced responses of colliding structures. The examined cases in the study clearly indicated that the induced responses due to collisions are not noticeably sensitive to the variation of the stiffness values of the impact element. In the same study, the influence of variations of damping values of the impact element on the induced responses has also been assessed and found to be insensitive as well. In addition, Jankowski (2007) carried out an experimental study in order to determine the range the impact stiffness parameter and the coefficients of restitution for structural pounding between the most commonly used building materials, such as: steel, concrete, and timber. Moreover, several previous studies indicated that changes in stiffness of impact element slightly affects responses of colliding structures (Anagnostopoulos and Spiliopoulos 1992, Maison and Kasai 1992, Kim *et al*. 2000, Abdel Raheem *et al*. 2019a, b).

4.2 Equations of motion considering sloshing force

The dynamic equation of motion of the building models shown in Fig. 1(b) considering the effect of sloshing force $\boldsymbol{F_s}$ can be written as follows

$$\begin{pmatrix} \boldsymbol{M^L} & \boldsymbol{O} \\ \boldsymbol{O} & \boldsymbol{M^R} \end{pmatrix}\begin{pmatrix} \ddot{\boldsymbol{U}}^{\boldsymbol{L}} \\ \ddot{\boldsymbol{U}}^{\boldsymbol{R}} \end{pmatrix} + \begin{pmatrix} \boldsymbol{C^L} & \boldsymbol{O} \\ \boldsymbol{O} & \boldsymbol{C^R} \end{pmatrix}\begin{pmatrix} \dot{\boldsymbol{U}}^{\boldsymbol{L}} \\ \dot{\boldsymbol{U}}^{\boldsymbol{R}} \end{pmatrix} + \begin{pmatrix} \boldsymbol{R^L} \\ \boldsymbol{R^R} \end{pmatrix} + \begin{pmatrix} \boldsymbol{P} \\ -\boldsymbol{P} \end{pmatrix} + \begin{pmatrix} \boldsymbol{F_S^L} \\ \boldsymbol{F_S^R} \end{pmatrix} = -\begin{pmatrix} \boldsymbol{M^L} & \boldsymbol{O} \\ \boldsymbol{O} & \boldsymbol{M^R} \end{pmatrix}\begin{pmatrix} \ddot{\boldsymbol{U}}_{\boldsymbol{g}} \\ \ddot{\boldsymbol{U}}_{\boldsymbol{g}} \end{pmatrix} \tag{4}$$

The elements of the sloshing force vectors of left and right buildings can be written as follows

$$\boldsymbol{F_S^L}=\begin{pmatrix} 0 \\ 0 \\ f_s^l \end{pmatrix}, \boldsymbol{F_S^R}=\begin{pmatrix} 0 \\ 0 \\ f_s^r \end{pmatrix} \tag{5}$$

The value of f_s can be calculated using Eq. (6). As (Reed *et al*. 1988)

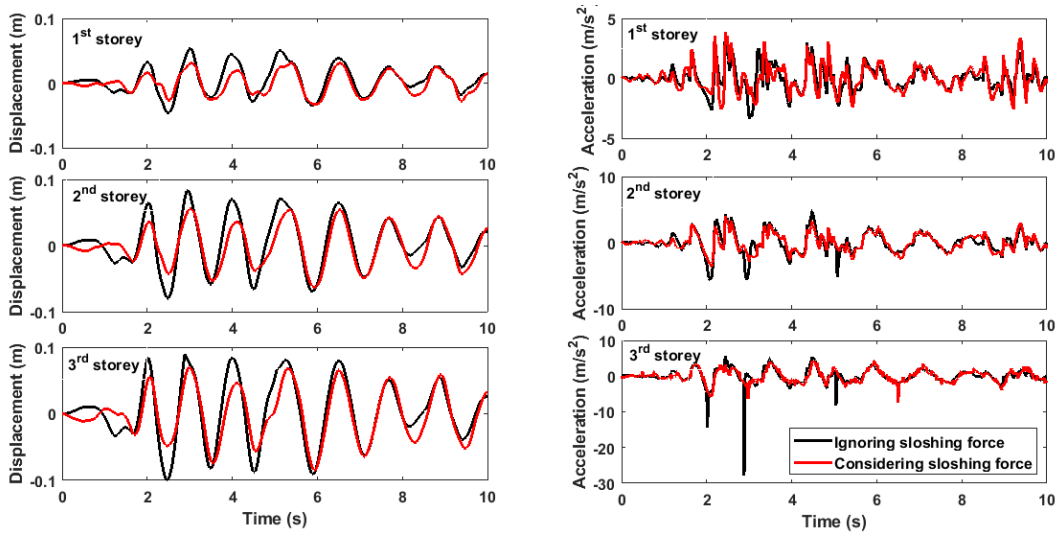

Fig. 3 Displacement and acceleration response time-histories under the El-Centro earthquake for the flexible building with and without the sloshing force effect

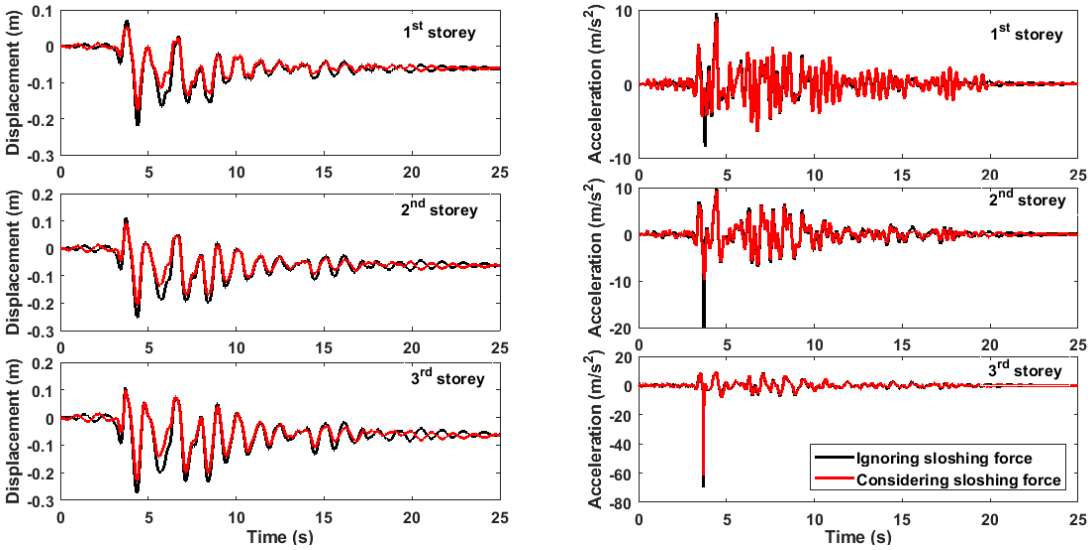

Fig. 4 Displacement and acceleration response time-histories under the Kobe earthquake for the flexible building with and without the sloshing force effect

$$f_S = \frac{1}{2}\rho g B(h_{wr}^2 - h_{wl}^2) \quad (6)$$

where, B, h_{wr} and h_{wl} are the width of the water tank and the instantaneous wave heights at the end wall on the right and left sides, respectively.

4.3 Solution procedure for equations of motion

For the purpose of performing many dynamic simulations with and without pounding incidences considering and ignoring sloshing force effects, a software application utilizing the MATLAB programming language was specifically developed. The developed code is mainly depending on the FE toolbox CALFEM. The developed code solves numerically Eqs. (1) and (4) over a time interval specified by the user employing the step 2 function in the toolbox. The developed function uses the step-by-step Newmark family methods with constant coefficients γ and β, which can be set by the user. The average acceleration approach is employed herein with γ=0.5 and β=0.25 over a small-time interval to achieve unconditional stability.

5. Numerical results and discussion

Two different configurations of the adjacent buildings are considered for performing the simulation analysis. First configuration is comprised of two adjacent buildings having three-story and the second configuration is comprised of two adjacent three-story buildings with water tanks attached at the top of the buildings. The parameters of the stories of the left building are chosen to ensure flexible building while the parameters of the stories of the right building are chosen such that the building behaves as a stiff one. The left building is supposed to be residential buildings with 25-ton mass per story and fundamental natural period of 1.2 s. The

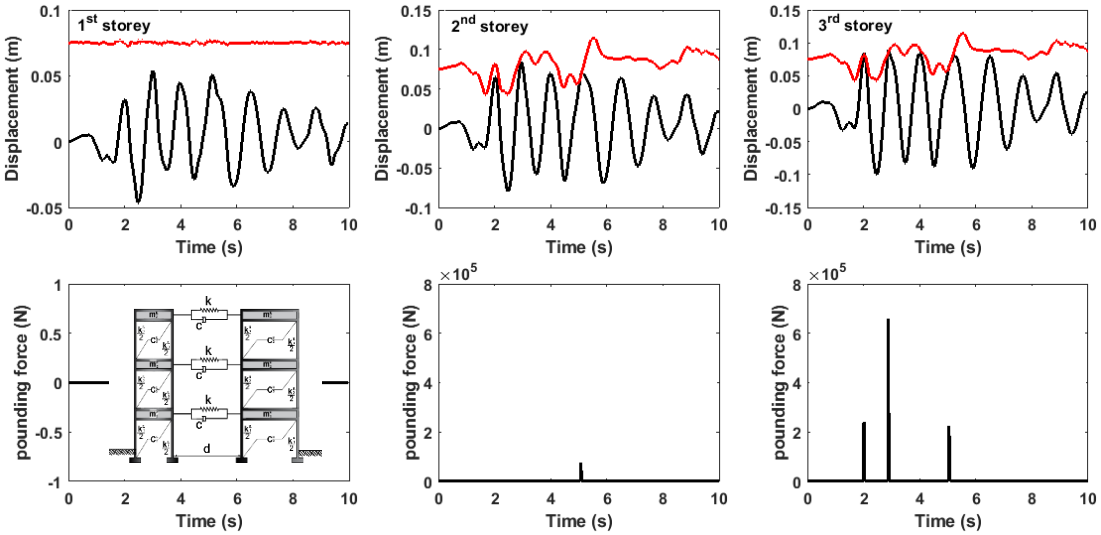

Fig. 5 Displacement and corresponding pounding force response time-histories under the El-Centro earthquake for the flexible and stiff buildings without the sloshing force effect

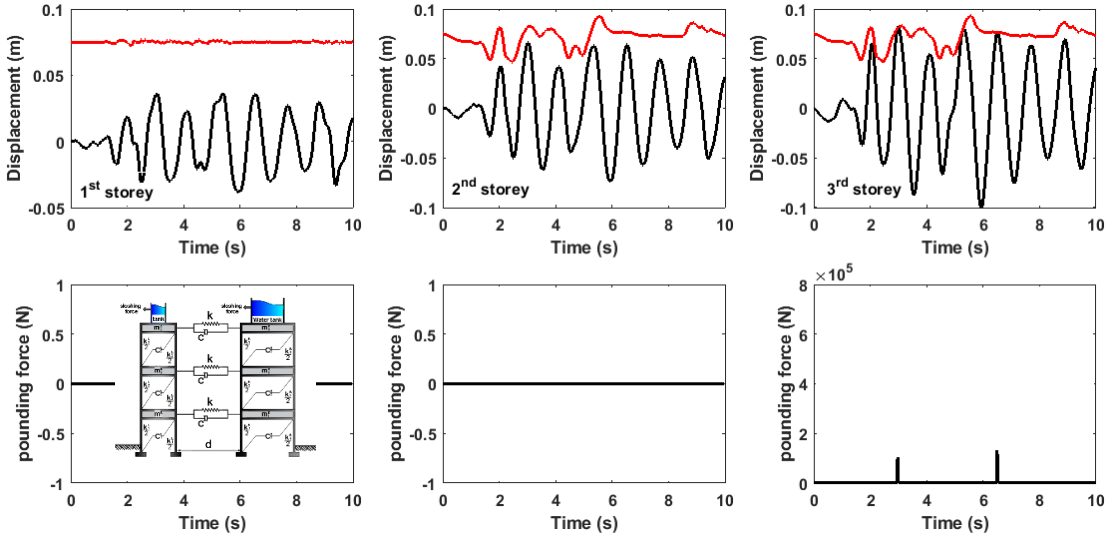

Fig. 6 Displacement and corresponding pounding force response time-histories under the El-Centro earthquake for the flexible and stiff buildings the sloshing force effect

right building has a mass of 1000 ton per story and fundamental period of 0.3 s. The selected natural periods clearly imply that the left building behaves in a flexible way while right building behaves in a stiff way. The sizes of the structural elements of the equivalent 3-storeyed models with roof water tanks monolithically attached at top in terms of columns, beams, and slabs are 900 mm×900 mm, 300 mm×600 mm and 140 mm respectively for the heavy and stiff building model. For the light and flexible building model the assigned sizes are 200 mm×200 mm, 120 mm×200 mm and 100 mm respectively. Two strong ground motion records are used to excite the two different building model configurations. The chosen records are near-fault with different PGAs from Kobe 1995-KJMA station and El-Centro 1940-117 El-Centro station. The seismic responses of the stories of building models in each configuration are computed, evaluated and discussed. In the case of pounding, the nonlinear viscoelastic model is employed, assuming coefficient of restitution of 0.6, and a value of impact stiffness equals to 2.75 GN/mm to be used in the simulation analysis.

Based on the obtained simulation results, the stories displacements as well as accelerations of the flexible building may significantly decrease due to the inclusion of sloshing force effect that occurs when a water tank is available at the top of the building. Figs. 3 and 4 provide the displacement and acceleration time histories under the El-Centro and Kobe earthquake records for the flexible building without and with a roof water tank. It can be seen from the figures that, under the two ground motions the obtained displacement of the stories ignoring the sloshing force effect are relatively higher than those of stories considering the sloshing force effect. Similarly, High values of acceleration response are observed at the time of ignoring the sloshing effect compared with acceleration response values of the floors of neighbouring buildings with

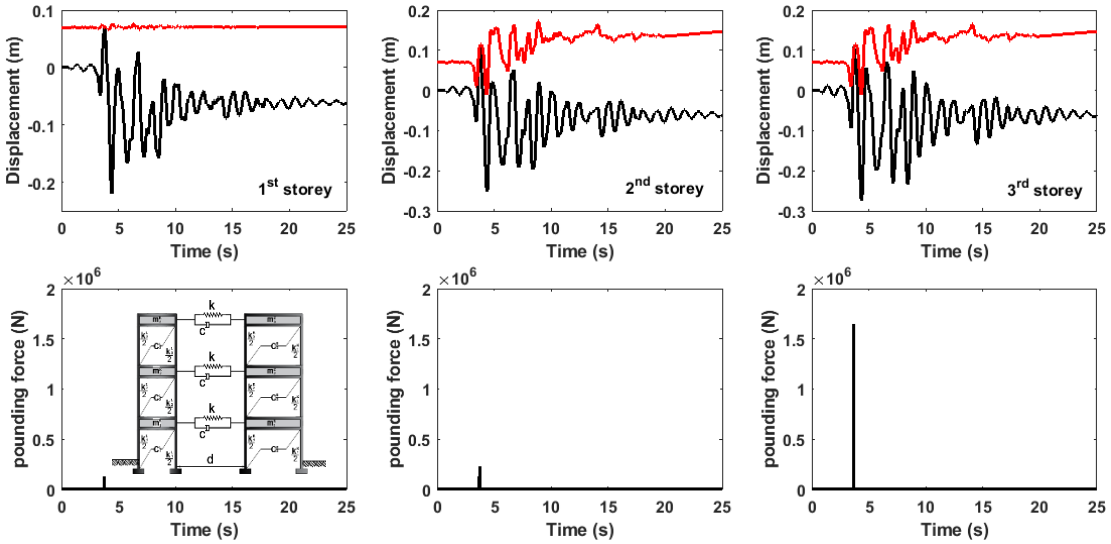

Fig. 7 Displacement and corresponding pounding force response time-histories under the Kobe earthquake for the flexible and stiff buildings without the sloshing force effect

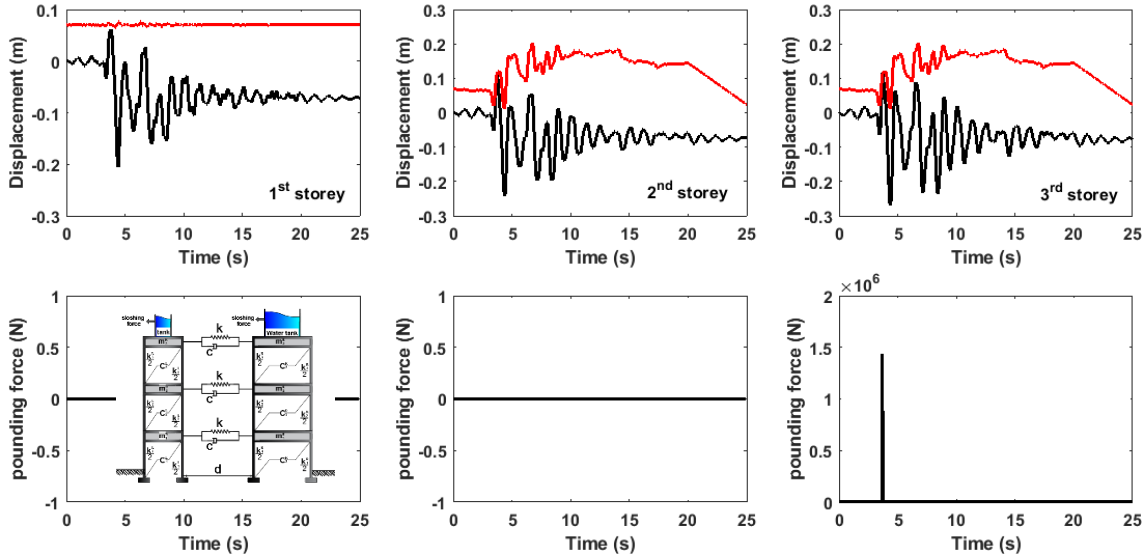

Fig. 8 Displacement and corresponding pounding force response time-histories under the Kobe earthquake for the flexible and stiff buildings the sloshing force effect

water tanks. It can also be seen from the figures that; such inclusion of the sloshing force significantly decreases the magnitude and number of spikes that appear in the acceleration time-history without sloshing effect. This implies that considering the effect of sloshing force due to the existence of a water tank alters the response of structures subjected to earthquake excitations. The overall results obtained from exciting the flexible building indicate that the responses of the building are considerably influenced by the existence of a water tank.

The influence of employing the effect of roof water tanks is further substantiated with respect to the utilized herein ground motion records time-histories. Here, responses of adjacent buildings modelled as MDOF systems shown in Fig. 1 in terms of story displacements and the corresponding pounding force time-histories are investigated. The numerical simulations are first conducted for the case without considering the existence of water tanks over the neighbouring buildings then the simulations are repeated incorporating such existence in order to clarify the role of the induced sloshing force under seismic actions. The results for this analysis for the stories of both buildings under the El-Centro and Kobe ground motion records are plotted in Figs. 5-8. The captured seismic responses of the adjacent buildings system without the inclusion of the effect of sloshing force are significantly different comparing to the seismic responses of the system considering the effect of sloshing force. More specifically, the induced pounding forces at each story level are significantly different considering the two states (compare Figs. 5 and 6 for the El-Centro and Figs. 7 and 8 for the Kobe earthquake as seismic excitations). For the case of the adjacent buildings system modelled without water tanks attached to the top floors, the first collision occurs at the stories of second level under the

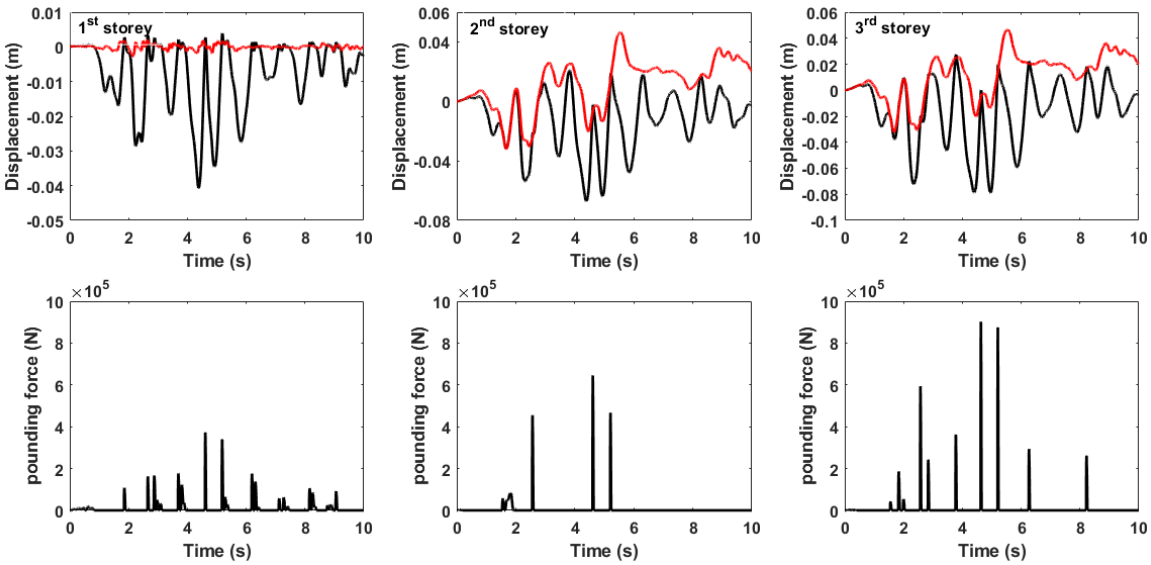

Fig. 9 Displacement and corresponding pounding force response time-histories under the El-Centro earthquake for the flexible and stiff buildings without the sloshing force effect for contact from the beginning (d=0)

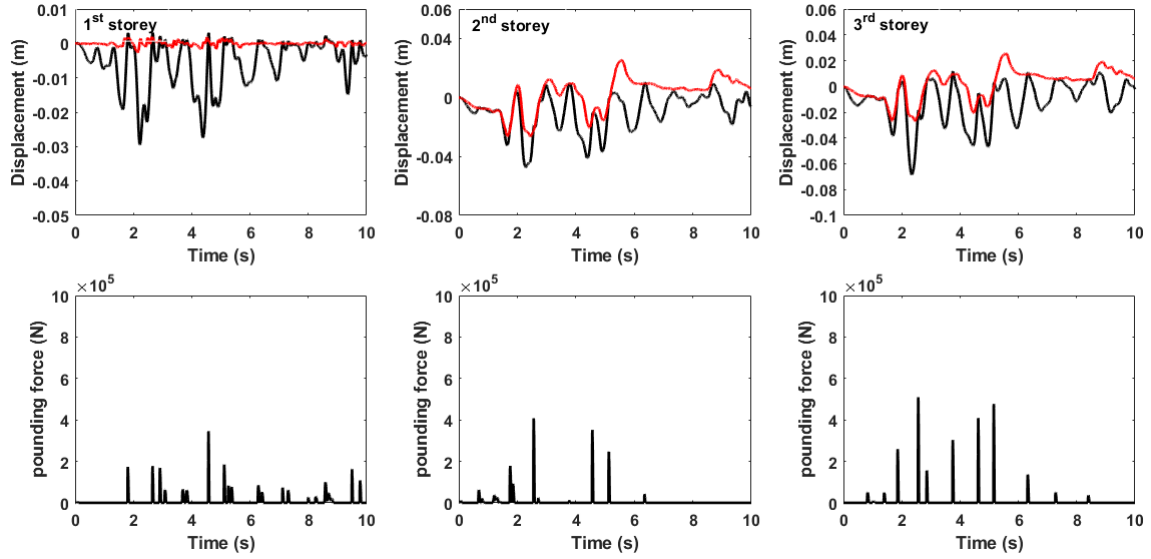

Fig. 10 Displacement and corresponding pounding force response time-histories under the El-Centro earthquake for the flexible and stiff buildings the sloshing force effect for contact from the beginning (d=0)

El-Centro records and at the stories of first level under the Kobe ground motion records considered in the study (see Fig. 5 and Fig. 7). In addition to collision between stories at second level, the adjacent buildings tend to pound together in several times at the stories of third level. As can be seen from Fig. 5, the third level stories of the flexible and stiff buildings collide three times under the El-Centro earthquake as seismic load if the effect of roof water tanks is ignored. For Kobe earthquake results, stories of the flexible and stiff buildings at third level come into contact for only one time as can be seen from Fig. 7. This can be due to the substantial movement into opposite direction of the flexible building is big enough to ensure that entering the yielding range and stories do not come into contact again. In order to emphasize the effect of sloshing force on the induced seismic responses of the buildings, the El-Centro and Kobe records are used to excite the building systems again considering the existence of water tanks over the buildings and the simulation results are presented in Figs. 6 and 8 respectively. As it can be seen from the figures, the inclusion of the effect of sloshing force significantly changes the induced responses of the adjacent buildings under the considered two ground motion records. Such inclusion of sloshing force prevents the stories at the second level of the flexible and stiff buildings from collisions as compared to the case of ignoring the existence of water tanks. It can be seen from Fig. 6 that; the number of impacts and the magnitude of the induced pounding forces under the El-Centro records are smaller during the inclusion of sloshing force effect as compared to the case of ignoring such effect (compare Fig. 5 and Fig. 6). For the simulated pounding force time-histories results between the

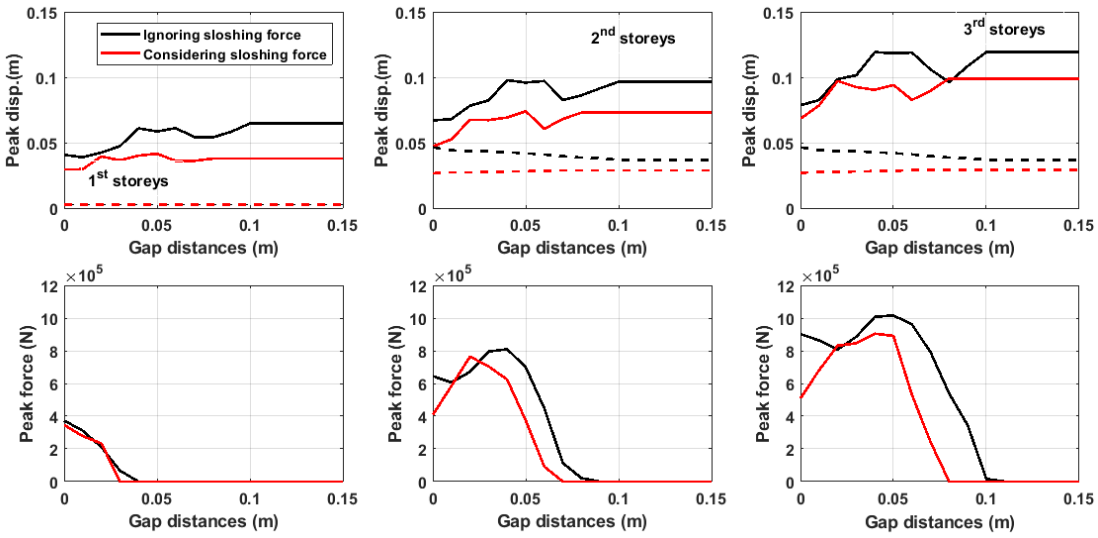

Fig. 11 Peak displacements and corresponding pounding forces against separation gap under the El-Centro earthquake for the flexible and stiff buildings with and without the sloshing force effect

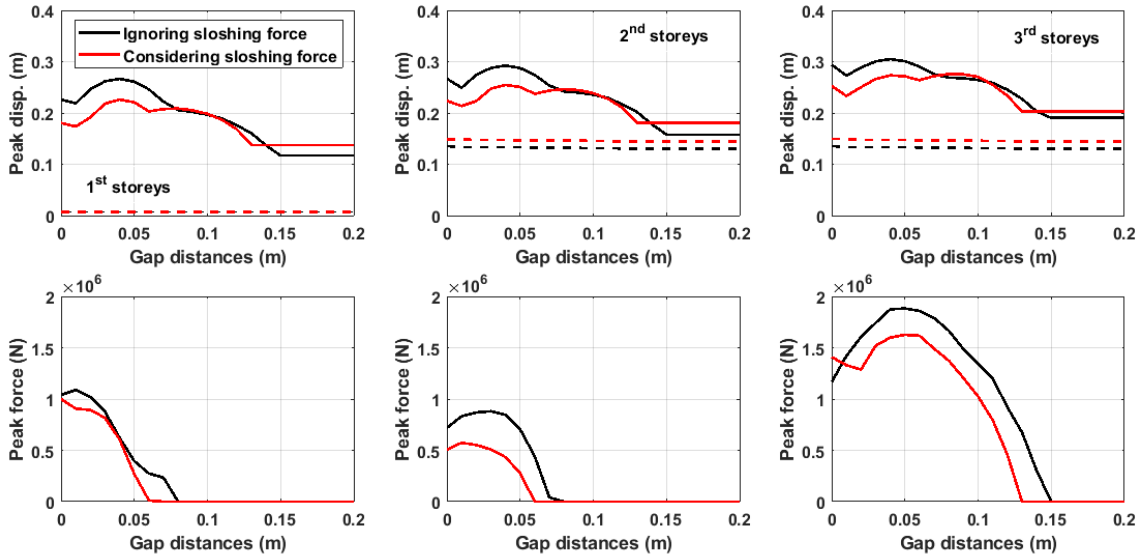

Fig. 12 Peak displacements and corresponding pounding forces against separation gap under the Kobe earthquake for the flexible and stiff buildings with and without the sloshing force effect

stories of the adjacent flexible and stiff buildings under the Kobe records, the inclusion of the sloshing force effect prevents occurrence of pounding between the stories of first level as well as stories at second level. The stories of the adjacent buildings at third level still collide with an induced pounding force of less magnitude than the one obtained due to the ignorance of roof water tanks effect. The obtained numerical results clearly indicate that the induced sloshing force under seismic actions due to the existence of roof water tanks prevents the lower stories from collisions, minimizes the number of impacts at higher stories, and reduces the magnitude of the induced pounding force due to collisions. Quantitively, for a specified insufficiently separation gap of 0.07 m between the neighbouring buildings, ignoring the inclusion of sloshing forces produces peak pounding force of value 0.75×10^5 kN, between stories at second level and 6.6×10^5 kN between stories of third levels under the El-Centro earthquake records. On the other hand, incorporating the sloshing effect decreases the induced peak pounding force value and allows impacting at only third level of value 1.31×10^5. The use of Kobe records produces impact force values of 0.13×10^6 kN, 0.23×10^6 kN, and 1.65×10^6 kN, at first, second, and third story levels ignoring the existence of the roof water tanks respectively. However, considering the sloshing effect decreases the induced peak pounding force value to 1.44×10^6 kN at only third story level. Incorporating the sloshing effect during collisions causes substantial decrease of the displacement response of the lighter and more flexible building. On the other hand, the displacement response of the heavier building is slightly affected. For example, the captured peak displacements for the case without incorporating the sloshing effect during collisions obtained for the first, the second and the third storey of the

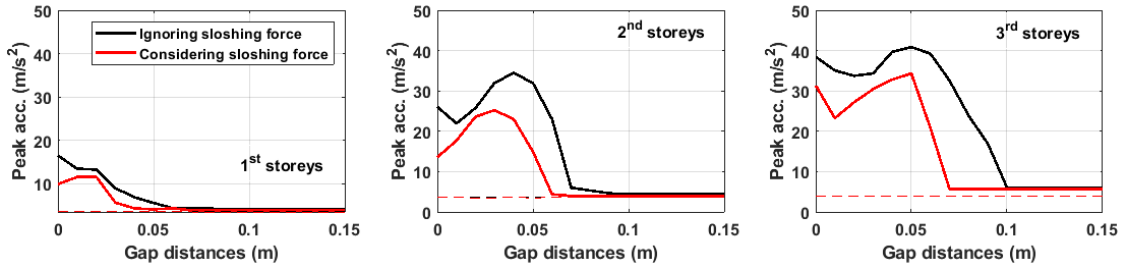

Fig. 13 Peak accelerations against separation gap under the El-Centro earthquake for the flexible and stiff buildings with and without the sloshing force effect

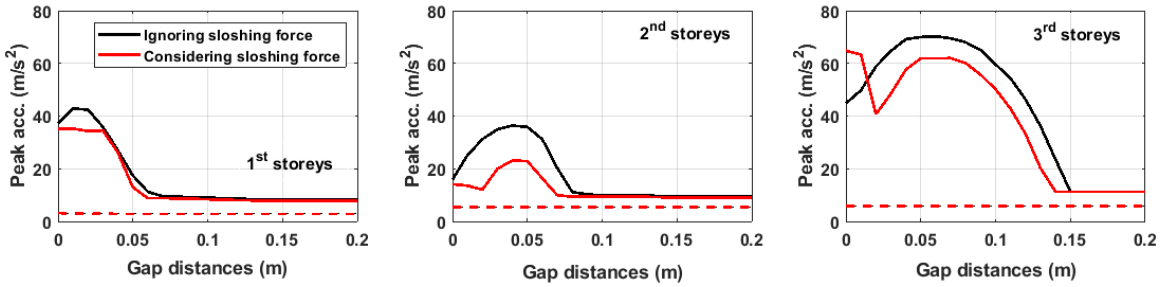

Fig. 14 Peak accelerations against separation gap under the Kobe earthquake for the flexible and stiff buildings with and without incorporating the sloshing force effect

left building under the El-Centro records are: 0.053, 0.084 and 0.10 m, respectively; while the corresponding values for the case ignoring such sloshing effect are: 0.032, 0.063 and 0.085 m, respectively. On the other hand, the storeys of the stiff right building induce peak displacements of: 0.003, 0.034 and 0.039 m incorporating the sloshing effect and without such incorporation produce peak displacements equal to: 0.003, 0.031 and 0.035 m for the first, the second and the third storey, respectively.

Further analysis to investigate the effect of roof water tanks on the induced displacements and the corresponding pounding forces for contact from the beginning (d=0) of the adjacent buildings with respect to the El-Centro records is presented in Figs. 9 and 10. The simulation figures introduce the induced story responses excluding and including the sloshing effect. As it can be seen from the figures, although the captured displacement and impact force responses excluding and excluding the effect of roof water tanks show different simulation results (compare Figs. 9 and 10 for the El-Centro earthquake as seismic excitations), setting the gap distance to be zero allows contacts to occur at all story levels either with or without roof water tanks. In addition, for the case of the adjacent buildings system modelled without water tanks, collision occurs at first, second and third story levels for several times. Considering the effect of water tanks does not prevent or even eliminate the number of collisions at the lower stories comparing to the case of initial gap d=7 cm. However, the inclusion of sloshing effect significantly reduces the magnitude of the induced displacements of the stories of flexible and stiff buildings as well as the captured pounding forces due to collisions. The values of the obtained numerical results of the induced peak pounding forces at first, second, and third story levels considering the effect of sloshing force are of values 3.45×10^5 kN, 4.08×10^5 kN, and 5.09×10^5 kN respectively. The corresponding results of the captured impact forces due to collisions ignoring the effect of existence of roof water tanks are of values 3.72×10^5 kN, 6.45×10^5 kN, and 9.02×10^5 kN respectively. These simulation values clearly clarify the role of roof water tanks in reducing the magnitude of induced forces due to collisions between adjacent buildings of zero separation distance.

The influence of the separation gap between the adjacent building without and with roof water tanks on the induced pounding-involved structural response is considered. The stories peak displacements are also considered through exciting the two adjacent building models with seismic gap varies from 0 to 0.2 m by the two different earthquake records. The plots in Figs. 11 and 12 present the peak responses of the 3-story buildings under the El-Centro and Kobe records against the width of the seismic gap considering and ignoring the effect of sloshing force. The simulation results indicate that the envelope of peak responses is considerably decreased for the used two simulation records due to the inclusion of the sloshing force effect. In general, the existence of water tanks at the top of adjacent structures reduces the value of seismic gap required to prevent pounding between the stories at different levels. In addition, the magnitude of the induced pounding forces is also reduced. For both including and excluding the effect of sloshing force, the obtained peak displacements of the stories of the flexible building increase as the seismic gap size increases and with further increase stories provide constant values under the El-Centro earthquake records. The obtained peak displacement results for the Kobe records show an increase trend up to a certain value of gap size followed by a decrease trend before providing nearly constant values of peak displacements as a result of end of collisions between stories due to wider

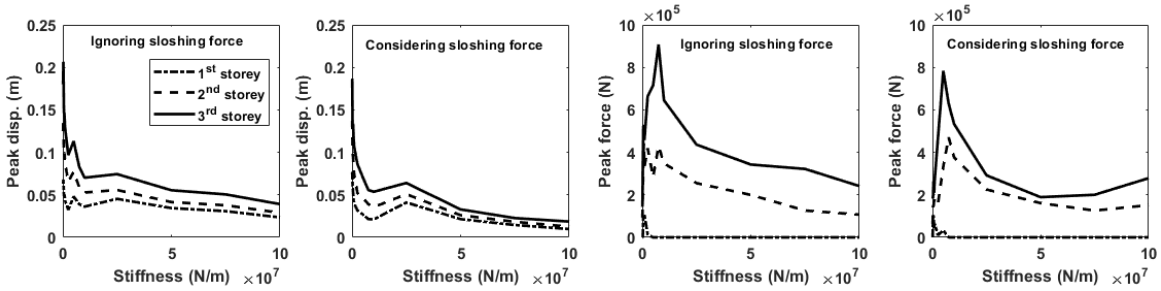

Fig. 15 Peak displacements and corresponding pounding forces against stiffness under the El-Centro earthquake for with and without the sloshing force effect

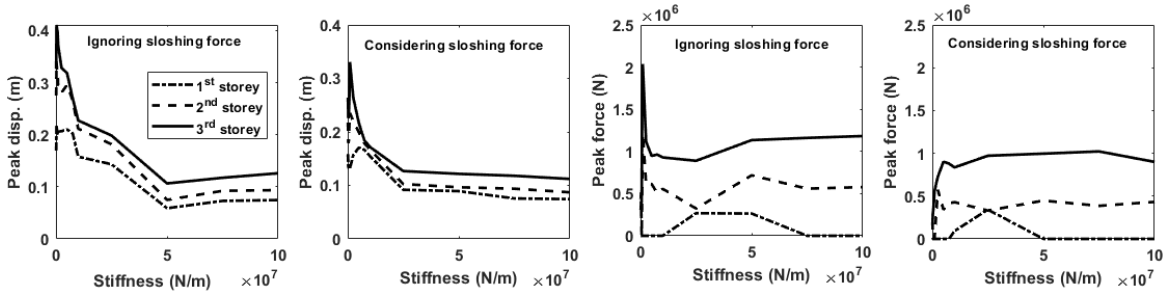

Fig. 16 Peak displacements and corresponding pounding forces against stiffness under the Kobe earthquake for with and without the sloshing force effect

seismic gaps. For the heavy and stiff buildings, it is observed that, in general, the computed maximum responses are very similar and very close where the stories produce nearly unchanged peak displacement values with the variation of the separation gap for the applied herein El-Centro and Kobe ground motion records respectively. Comparisons between the obtained peak pounding forces between stories considering and ignoring sloshing effect are also presented in Figs. 11 and 12. The plotted numerical results show that the inclusion of sloshing force effect requires narrower separation gap as compared to the case of ignoring such effect. Moreover, the inclusion of sloshing effect can reduce the peak pounding forces induced at the considered story levels compared with the case of ignoring such sloshing effect under the considered two earthquake excitations. As it can be seen from the figures, for the cases of including and excluding the sloshing effect, higher stories collide at wider gap sizes compared with lower stories for the simulation results under the El-Centro and Kobe. Moreover, with the increase in the provided seismic gap, the induced peak impact forces increase up to a certain maximum value. Further increase in the provided gap, the envelope of the produced pounding forces due to collisions tends to decrease.

Due to the proportionality of the exerted forces in the structures subjected to earthquake excitations with the developed floor accelerations, the MDOF building models are also considered herein for investigating the effect of sloshing forces on the story's accelerations. Several separation gaps, as influencing parameter, are purposely varied in order to assess how they affect the role of sloshing force on the induced accelerations of adjacent buildings during pounding. The peak accelerations of the stories of the adjacent building models are recorded for the cases without and with incorporating the effect of sloshing force for the applied herein ground motion records namely; the 1940 El-Centro and Kobe earthquake records respectively. As it can be seen from the Figs. 13 and 14, considering the effect of sloshing usually leads to the decrease in the peak accelerations of the stories of flexible building for all the considered gap size values during collisions compared with the case of ignoring existence of water tanks. The results also indicate that, as the gap size increases, the obtained story's peak accelerations of the flexible building increase up to a certain maximum value and with further increase in the gap size a decrease trend can be observed for with and without inclusion of sloshing effect. Then, with further increase in the seismic separation distance, the calculated story's peak acceleration values remain nearly unchanged. Moreover, the induced stories accelerations of the heavy and stiff building seem to be insensitive to the variation of the provided seismic gap as well as the inclusion of the sloshing force effect where the obtained values are almost constant and identical.

The obtained simulation results of the storey peak displacements and forces for different values of the storey stiffness for the cases without and with the sloshing force effect under both the El-Centro and Kobe records, respectively are shown in Figs. 15 and 16. It can be seen that the obtained peak displacement and the corresponding peak force responses differ greatly with the variation of storey stiffness. The captured peak displacement values show a decrease trend with the increase of the storey stiffness. Further increase in the stiffness values show steadily decreasing slope in the obtained peak displacements for including and excluding the effect of existence of roof water tanks. However, the results from both earthquakes show that the buildings come into contact

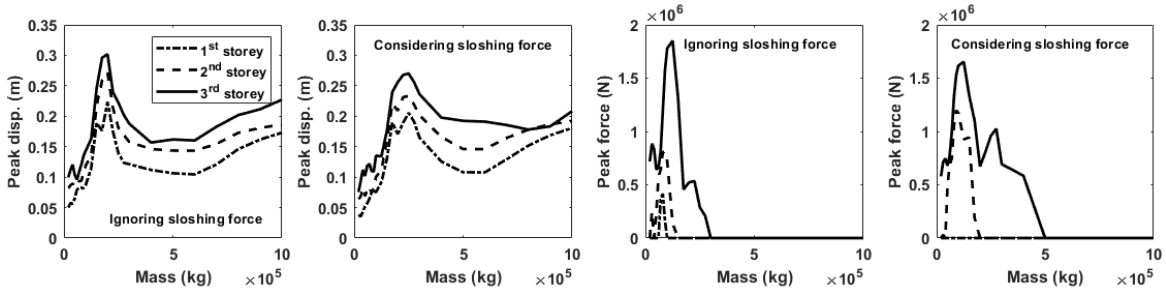

Fig. 17 Peak displacements and corresponding pounding forces against mass under the El-Centro earthquake for with and without the sloshing force effect

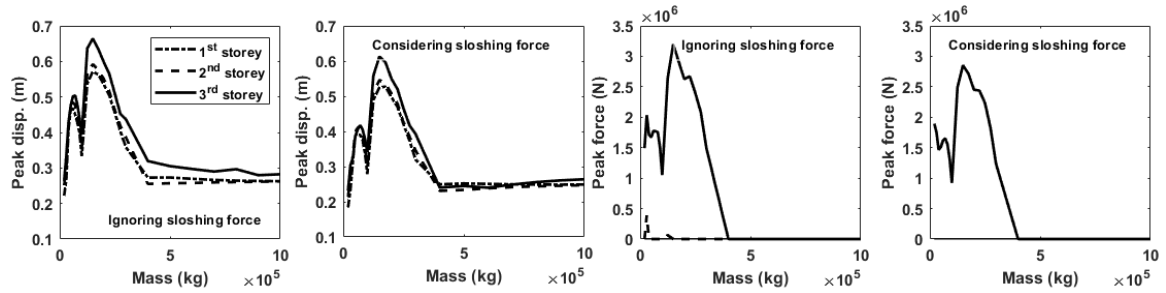

Fig. 18 Peak displacements and corresponding pounding forces against mass under the Kobe earthquake for with and without the sloshing force effect

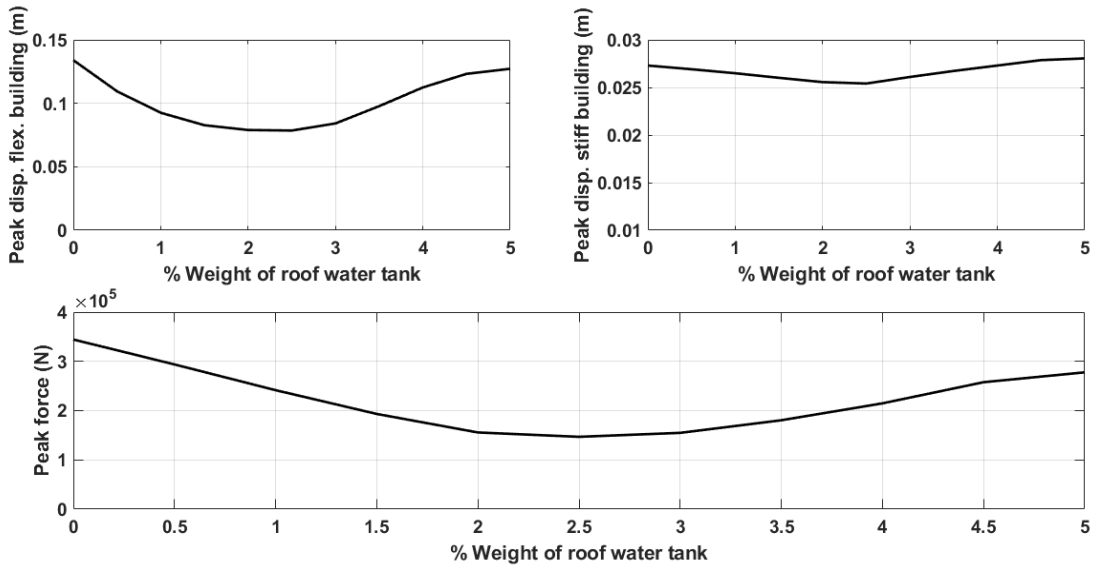

Fig. 19 Variation of the peak displacements and corresponding pounding forces against percentage of water under the El-Centro earthquake records

for all the considered stiffness values as can be observed from the figures. In case of pounding force response, the trend of peak force responses under the El-Centro earthquake records show substantial increase at lower stiffness values followed by a decrease trend with the increase in the storey stiffness values. The observed trend for the peak forces under the Kobe records is quite similar to the trend observed under the El-Centro records for the case that ignores the sloshing effect. However, including the sloshing effect shows slight influence of the variation of storey stiffness values on the induced peak forces. In addition, such inclusion of sloshing effect removes the substantial increase of the induced peak forces at lower stiffness values under Kobe earthquake records of higher PGA.

The obtained simulation results of peak displacements and the corresponding peak forces of storeys due to the variation of the mass, as an important dynamic characteristic parameter, are shown in Figs. 17 and 18 under the applied El-Centro and Kobe earthquake records respectively. As it can be seen from the figures, the incorporation of sloshing effect reduces the values of the induced peak displacements and forces with the variation in the considered storey masses. The plotted results also

clearly indicate that the change of the considered building mass significantly influences the induced responses. A general trend under the considered two ground motion records shows an increase in the captured peak displacements as the storey masses increase up to a certain limit. With further increase in the storey masses a decrease trend can be observed followed by nearly unchanged peak displacement values under the Kobe records. However, the peak displacement results under the El-Centro records follows a steadily increasing slope with the increase in storey mass values. The induced peak pounding forces almost follow the same trend as the obtained peak displacements. As it can be seen from the figures, as the storey masses get increase the induced peak forces diminish.

In order to investigate the influence of quantity of water in roof tank on the induced seismic responses during collisions, the amount of water was varied in the roof tank and the peak displacements and impact forces were recorded and presented in Fig. 19. The displacement and pounding force responses were maximum with empty water tank. The obtained responses in terms of displacement and impact force gradually decrease with increase of the percentage of weight of roof water tank, i.e., increase of the quantity of water in the tank, till reaching an optimum value. With further increase in the percentage weight of tank, the captured responses start a gradual increase. The optimum percentage value of added water in tank at the top of the flexible building was around 2% of the light building weight. Although the stiff building seems to be slightly affected, an optimum percentage value of about 2.5% of the stiff building weight. Similar pattern of results has been recorded for the variation of the induced pounding forces with the percentage weight of water to fill the roof water tank. However, the optimum percentage value of water required to produce lowest impact forces has been found to be in the range of 2.0%-3.0% of the weight of the buildings. This can be due to the induced pounding force mainly depends on the characteristics of the adjacent two buildings

6. Conclusions

Based on the results from numerical simulations of the potential of using the roof water tanks as a mitigation measure to minimize the required separation gap and induced pounding forces due to collisions, it could be concluded that roof water tanks are beneficial in reducing the magnitude of induced pounding forces several times due to collisions from the beginning, (d=0), or collisions with provided insufficient separation gap, (i.e., d=0.07 m). In addition, the number of resulting impacts between stories has been reduced particularly for the insufficient gap case. moreover, the existence of water tanks can be a viable alternative to minimize the gap distance recommended by the seismic design codes. The response quantities in terms of story displacements and accelerations have been reduced noticeably under earthquake excitations when the water tanks are attached to the top of the structure compared with the case of adjacent buildings without roof water tanks. Existence of roof water tanks during earthquake excitations can reduce or even eliminates the generated high, short-duration, acceleration spikes which may cause damage of non-structural elements. The obtained numerical results of the performed parametric investigation confirm that the change in the considered different structural parameters, such as separation gap between buildings, story mass, and structural stiffness significantly affects the induced peak responses during collisions with and without roof water tanks. The induced responses of stories of flexible building are more sensitive and totally affected by the existence of roof water tanks in comparable with the response of stories of stiff building under earthquake vibrations. The amount of water in the range of 2.0% to 3.0% with reference to the weight of buildings provides the optimum effect of roof water tanks to mitigate the displacement and pounding force responses during the occurrence of ground accelerations.

References

Abdeddaim, M., Ounis, A. and Djedoui, N. (2016), "Pounding hazard mitigation between adjacent planar buildings using coupling strategy", *J. Civil Struct. Hlth. Monit*., **6**(3), 603-617. https://doi.org/10.1007/s13349-016-0177-4.

Abdel Mooty, M.N. and Ahmed, N.A, (2017), "Pounding mitigation in buildings using localized interconnections", *The 2017 World Congress on Advances in Structural Engineering and Mechanics - AEM17 Seoul*, Korea.

Abdel Raheem, S.E, Fooly, M.Y.M., AbdelShafy, A.G.A., Abbas, Y.A., Omar, M., Taha, A.M. and AbdelLatif, M.M.S. (2019a), "Numerical simulation of potential seismic pounding among adjacent buildings in series", *Bull. Earthq. Eng*., **17**(1), 439-471.

Abdel Raheem, S.E. (2014), "Mitigation measures for earthquake induced pounding effects on seismic performance of adjacent buildings", *Bull. Earthq. Eng*., **12**(4), 1705-1724.

Abdel Raheem, S.E., Ahmed, M.M.M., Ahmed, M.M. and Abdel-Shafy, A.G.A. (2018a), "Evaluation of plan configuration irregularity effects on seismic response demands of L-shaped MRF buildings", *Bull. Earthq. Eng*., **16**(9), 3845-3869.

Abdel Raheem, S.E., Fooly, M.Y.M., AbdelShafy, A.G.A., Abbas, Y.A., Omar, M., Taha, A.M., AbdelLatif, M.M.S. and Mahmoud, S. (2018b), "Seismic pounding effects on adjacent buildings in series with different alignment configurations", *Steel Compos. Struct.*, **28**(3), 289-308.

Abdel Raheem, S.E., Fooly, Y.M.F., Omar, M. and Abdel Zaher, A.K. (2019b), "Seismic pounding effects on the adjacent buildings with eccentric alignment", *Earthq. Struct.*, **16**(6), 715-726.

Abdullah, M., Hanif, J.H., Richardson, A. and Sobanjo, J. (2001), "Use of a shared tuned mass damper (STMD) to reduce vibration and pounding in adjacent structures", *Earthq. Eng. Struct. Dyn*., **30**(8), 1185-1201.

Anagnostopoulos, S. and Spiliopoulos, K. (1992), "An investigation of earthquake induced pounding between adjacent buildings", *Earthq. Eng. Struct. Dyn*., **21**, 289-302.

Anagnostopoulos, S.A. (1988), "Pounding of buildings in series during earthquakes", *Earthq. Eng. Struct. Dyn*., **16**(3), 443-456.

Anagnostopoulos, S.A. and Karamaneas, C.E. (2008), "Use of collision shear walls to minimize seismic separation and to protect adjacent buildings from collapse due to earthquake-induced pounding", *Earthq. Eng. Struct. Dyn*., **37**, 1371-1388.

Cao, L. and Li C. (2019), "Tuned tandem mass dampers-inerters with broadband high effectiveness for structures under white noise base excitations", *Struct. Control Hlth. Monit.*, **26**(3),

e2319. https://doi.org/10.1002/stc.2319.
Dyke, S.J., Spencer, B.F., Sain, M.K. and Carlson, J.D. (1998), "An experimental study of MR dampers for seismic protection", *Smart Mater. Struct.*, **7**(5), 693-705.
Elwardany, H., Seleemah, A. and Jankowski, R. (2017), "Seismic pounding behavior of multi-story buildings in series considering the effect of infill panels", *Eng. Struct*., **144**(1), 1201-1217.
Favvata, J.M., Karayannis, C.G. and Liolios, A.A. (2009), "Influence of exterior joint effect on the inter-story pounding interaction of structures", *Struct. Eng. Mech.*, **33**(2), 113-136.
GRM (2009), M6.3 L'Aquila, Italy, Earthquake Field Investigation Report, Global Risk Miyamoto, Sacramento, California, USA.
Guenidi, M.Z., Abdeddaima, M., Ounisa, A., Shrimali, M.K. and Datta, T.K. (2017), "Control of adjacent buildings using shared tuned mass damper", *Procedia Eng.*, **199**, 1568-1573.
Jankowski, R. (2005), "Non-linear viscoelastic modelling of earthquake-induced structural pounding", *Earthq. Eng. Struct. Dyn*., **34**, 595-611.
Jankowski, R. (2007), "Theoretical and experimental assessment of parameters for the non-linear viscoelastic model of structural pounding", *J. Theo. Appl. Mech.*, **45**(4), 931-942.
Jankowski, R. (2008), "Earthquake-induced pounding between equal height buildings with substantially different dynamic properties", *Eng. Struct*., **30**, 2818-2829. https://doi.org/10.1016/j.engstruct.2008.03.006.
Jankowski, R. and Mahmoud, S. (2016), "Linking of adjacent three-storey buildings for mitigation of structural pounding during earthquakes", *Bull. Earthq. Eng*., **14**(11), 3075-3097.
Karayannis, C.G. and Favvata, M.J. (2005a), "Inter-story pounding between multistory reinforced concrete structures", *Struct. Eng. Mech.*, **20**(5), 505-526.
Karayannis, C.G. and Favvata, M.J. (2005b), "Earthquake-induced interaction between adjacent reinforced concrete structures with non-equal heights", *Earthq. Eng. Struct. Dyn.*, **34**, 1-20.
Karayannis, C.G. and Naoum, M.C. (2018), "Torsional behavior of multistory RC frame structures due to asymmetric seismic interaction", *Eng. Struct.,* **163**, 93-111.
Kasai, K. and Maison, B.F. (1997), "Building pounding damage during the 1989 Loma Prieta Earthquake", *Eng. Struct.*, **3**(19), 195-207.
Kim, S.H., Lee, S.W and Mha, H.S. (2000), "Dynamic behaviors of the bridge considering pounding and friction effects under seismic excitations", *Struct. Eng. Mech.*, **10**, 621-633.
Komodromos P, Polycarpou PC, Papaloizou L and Phocas MC. (2007), "Response of seismically isolated buildings considering poundings", *Earthq. Eng. Struct. Dyn*., **36**, 1605-1622.
Mahmoud, S. and Gutub, S. (2013), "Earthquake induced pounding-involved response of base-isolated buildings incorporating soil flexibility", *Adv. Struct. Eng.*, **16**(12), 71-90.
Mahmoud, S. and Jankowski, R. (2010), "Pounding-involved response of isolated and non-isolated buildings under earthquake excitation", *Earthq. Struct*., **1**(3), 3250-3262.
Mahmoud, S., Abdelhameed, A. and Jankowski R. (2013), "Earthquake-induced pounding between equal height multi-storey buildings considering soil-structure interaction", *Bull. Earthq. Eng*., **11**(4), 1021-1048.
Mahmoud, S., Genidy, M. and Tahoon, H. (2017), "Time-history analysis of reinforced concrete frame buildings with soft storeys", *Arab. J. Sci. Eng.*, **42**(3), 1201-12017.
Maison, B.F. and Kasai, K. (1992), "Dynamics of pounding when two buildings collide", *Earthq. Eng. Struct. Dyn*., **21**, 957-77.
Moustafa, A. and Mahmoud, S. (2014), "Damage assessment of adjacent buildings under earthquake loads", *Eng. Struct.*, **61**, 153-165.
Reed, D.A., Yu, J., Yeh, H. and Gardarsson, S. (1998), "Investigation of tuned liquid dampers under large amplitude excitation", *J. Eng. Mech.*, **124**(4), 405-413.
Rosenblueth, E. and Meli, R. (1986), "The 1985 Earthquake: causes and effects in Mexico City", *Concrete Int.*, ACI, **5**(8), 23-36.

AT